

Demonstration of a 0.54 Picosecond X-Ray Streak Camera

Z. Chang, A. Rundquist, H. Wang, M.M. Murnane, H.C. Kapteyn
Center for Ultrafast Optical Science
The University of Michigan
Ann Arbor, MI 48109-2099

Phone: (313) 763-0573; FAX: (313) 763-4876; E-mail: kapteyn@eecs.umich.edu

X. Liu, B. Shan, J. Liu, L. Niu, M. Gong, X. Zhang
State Key Laboratory of Transient Optics Technology,
Xi'an Institute of Optics and Precision Mechanics, Xi'an, 710000, P. R. China

R. Lee
Lawrence Livermore National Laboratory, Livermore, CA94551

Abstract

A magnetically focused x-ray streak camera was designed and tested using sub-20fs soft-x-ray pulses generated by high harmonic emission in a gas. The temporal resolution of the camera was demonstrated to be under 0.54 ps for the ultraviolet and 0.88 ps in the soft-x-ray wavelength region. Our streak camera represents the fastest x-ray detector developed to date, and should allow sub-picosecond time resolution experiments to be performed using either synchrotron or laser-plasma-based x-ray sources.

Keywords: streak camera, x-ray, sub-picosecond, high-harmonic generation

1. Introduction

During the past decade, the development of ultrafast x-ray sources based on laser-produced plasmas,[1] high harmonic emission in gases,[2,3] and synchrotron sources, has advanced rapidly. It is now possible to generate sub-picosecond pulses throughout the ultraviolet (uv), vacuum ultraviolet (vuv) and x-ray region of the spectrum, and the use of harmonic emission has resulted in the generation of soft-x-ray pulses as short as 10 fs.[4] However, progress in the development of ultrafast sub-picosecond x-ray detectors, such as x-ray streak cameras, has been relatively slower.[5,6] Although cross-correlation techniques have demonstrated femtosecond time resolution, such measurements are very difficult, and are possible only at discrete wavelengths.[7] The fastest x-ray streak camera measurement to date was demonstrated to be 2ps. This measurement was limited both by the time response of the streak camera itself, and by the laser-plasma-based x-ray source.[5,6] Such test pulses are far from ideal for fast streak camera calibration because their duration can be comparable to the resolution of the instrument being tested. In this letter we describe the design and implementation of a novel x-ray streak camera, which exhibits sub-picosecond time resolution. The time response of the streak camera was measured using ultrashort 10 fs high-order harmonics generated by 25 fs laser pulses.[4,8] The single shot response of our camera was experimentally demonstrated to be 0.88 ps.

2. Time resolution calculation

It is well known[9] that the temporal resolution of streak cameras is limited mainly by the transit-time dispersion of the photoelectrons as they travel from the photocathode to the deflection plates. It is also limited by the spatial resolution of the electron optics in the camera, and the deflection speed of the streak plates. For sub-picosecond time resolution, space charge effects may also limit the time resolution, and thus limit the dynamic range. For our work, we designed and tested a novel streak camera design, to reduce the limitations on temporal resolution as much as possible. The configuration of the new x-ray streak camera is shown schematically in Fig. 1. In our camera, a pair of meander-type deflection plates is located before a magnetic focusing lens. This has several advantages: first the electron transit time from the anode to the deflection plates is minimized, as is the transit time dispersion; second, the fast time response and high deflection sensitivity (8 cm/kV) of the meander type deflection plates provides the possibility of high sweep speeds on the exit phosphor screen; finally, the short transit time also reduces space charge effects. In addition to the use of meander type deflection plates to increase the time response, we also used a 20 μm x 5 mm slit, which was constructed as part the anode. This slit defined the field of view of the camera, and therefore no slit was needed at the photocathode. The use of a slit resulted in a higher throughput when compared with a standard acceleration mesh, typically used in streak cameras, and also results in a higher dynamic range for the instrument.

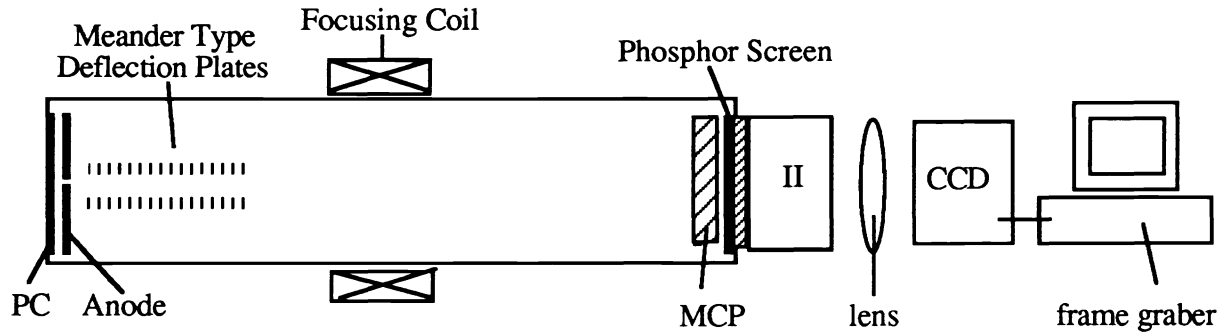


Figure 1: The configuration of the sub-picosecond X-ray streak camera.

The electron transit time dispersion from the photocathode to the deflection plates in the camera can be evaluated analytically. In the photocathode to anode region, the electric field can be treated as uniform, since the width of the slit in the anode is much smaller than the 1 mm space between the photocathode and anode. The transit time in this region can be calculated from[10] -

$$t_{pa} = \sqrt{\frac{2m}{e}} \frac{(\sqrt{V_o + V_a} - \sqrt{V_o})}{E} \quad (1)$$

where m and e are the charge and mass of the electron respectively, eV_o is the initial energy of an emitted photoelectron in the axial direction, V_a is the accelerating voltage, and E is the extraction field. Since $V_a \gg V_o$, from Eqn. (1) above we see that the transit time difference between an electron with initial energy eV_o and an electron with an initial energy of $V_o = 0$ is -

$$t'_{pa} = \sqrt{\frac{2mV_o}{e}} \frac{1}{E} \quad (2)$$

For x-ray photocathodes, the distribution of the initial energies of the emitted photoelectrons can be expressed as[11]

$$N(eV_o) = \frac{C(eV_o)}{(eV_o + W)^4} \quad (3)$$

where C is a constant, and W is related to the photocathode material. The photocathode material also determines $\delta\epsilon$, the FWHM of the energy distribution.

From Eqns. (2) and (3), we can obtain the transit time distribution of the electrons. The FWHM of this distribution is defined as the time dispersion, which can be shown to be -

$$\delta t_{pa} = \frac{2.63\sqrt{\delta\epsilon}}{E} \quad (\text{ps}) \quad (4)$$

where W and $\delta\epsilon$ are in eV, and E is in kV/mm. For our camera, the electric field between the photocathode (KBr) and anode is 10 kV/mm, resulting in a calculated time dispersion of about 276 fs.

The region between the anode and the entry to the deflection plates is nearly field free, and the transit time in this region is given approximately by -

$$t_{ad} = \frac{S}{\sqrt{\frac{2e}{m}(V_o + V_a)}} \quad (5)$$

where S is the length of this region. The transit time difference between an electron with initial energy eV_o and an electron with an initial energy of $V_o = 0$ is -

$$t'_{ad} \approx \sqrt{\frac{m}{8e}} \frac{SV_o}{V_a^{3/2}} \quad (6)$$

From Eqns. (6) and (2), we can obtain the transit time distribution of the electrons in this region, and the distribution FWHM -

$$\delta t_{ad} = \frac{1}{2} t_{ad} \frac{\delta \epsilon}{eV_a} \quad (7)$$

where $t_{ad} = S / (2eV_a/m)^{1/2}$ is the transit time for electrons with $eV_o = 0$. For our streak camera, $T_{ad} = 500$ ps, $V_a = 10$ kV, $\delta \epsilon = 1.1$ ev, so that δt_{ad} was calculated to be 25 fs.

It is clear that for our streak camera, the time dispersion in the anode-to-deflection plates region is much smaller than in the photocathode-to-anode region. This is because in the anode-deflection plate region, the electrons travel at high speeds, which reduces the relative speed difference, as seen from Eqn. (7). From (7) we also see that the dispersion is proportional to the transit time. In our camera, the transit time is 0.5 ns, which is much shorter than the commonly used static-electric field focused x-ray streak camera transit time of typically ≈ 4 ns. For such streak cameras, the time dispersion in both regions can be comparable.

The above analysis does not take into account the angular distribution of the photoelectrons emitted from the photocathode. We have however calculated the transit time dispersion from the photocathode to the deflection plates, assuming the angular distribution is Lambertian. The calculated dispersion, shown in Fig. 2, is 250 fs.

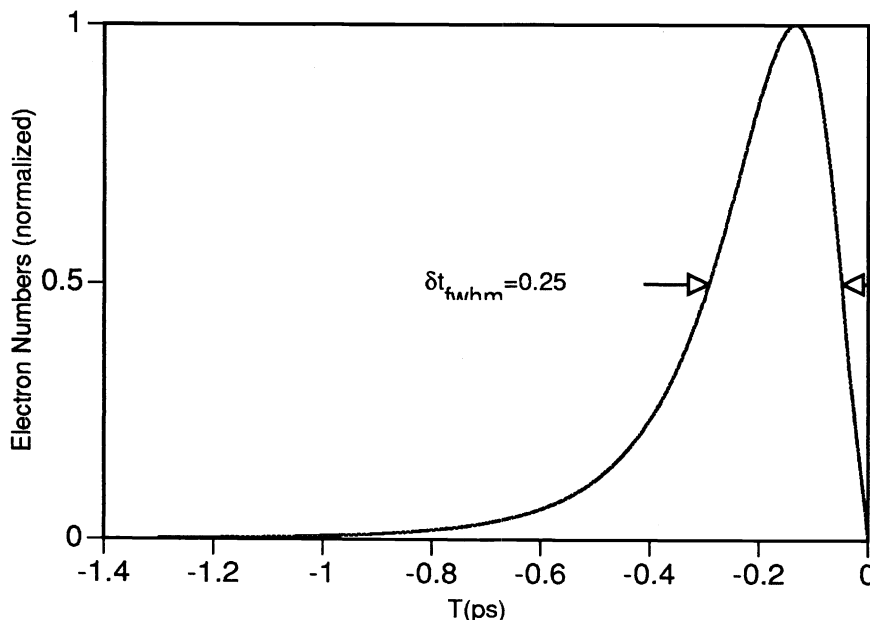


Fig.2 Calculated time dispersion from photocathode to deflection plates
(KBr photocathode, $E_a = 10$ kv/mm, $S = 30$ mm)

The spatial resolution of the streak tube was simulated by tracing the trajectories of the electrons from the photocathode to the phosphor screen. This was done by solving the dynamic equations of motion for the electrons in

an electromagnetic field, using the Runge-Kutta method. The magnetic field distribution was calculated by the finite difference method, assuming that the shield metal has an infinitely high magnetic permeability, and is not saturated. Our full numerical design of the streak camera allows us to improve the tube design, and our approach is much easier than the method based on measuring the magnetic field on axis.[12] The simulation shows that the point spread function of the image converter tube is not symmetric in the un-streaked mode. The width along the direction of the slit is larger than in the perpendicular direction due to the collimation effects of the slit. The calculated image width of the slit on the phosphor screen is $\approx 60 \mu\text{m}$.

In our camera, the photoelectrons are multiplied by a microchannel plate (MCP) detector placed in front of the phosphor screen, as shown in Fig 1. The output phosphor screen is fiber-optically coupled to a proximity focused second generation image intensifier. The image is then lens coupled to a low light CCD camera, which is connected to a frame grabber. The framing rate is about 3 Hz, which is limited by the speed of our Macintosh computer. The width of the slit image on the CCD camera is a convolution of the streak tube optics, the image intensifier, and the CCD camera. The experimentally measured width of the slit image is $\approx 80 \mu\text{m}$. The high voltage on the streak camera photocathode was applied by superimposing a - 5 kV pulse to a - 5 kV DC voltage. Use of a pulsed extraction field prevents electrical breakdown between the photocathode and the anode. A GaAs photoconductive switch[12] was used to obtain a fast ramp voltage for driving the deflection plates. This switch also exhibits a small relative time jitter of about 5 ps. The obtained sweep speed is $2 \times 10^8 \text{ m/s}$, so that the camera time resolution is limited at 400 fs by the spatial resolution and sweep speed. Taking into account the time dispersion also, the total estimated time resolution for our camera is $\approx 0.5 \text{ ps}$.

3. Experimental test

Since our x-ray streak camera is also sensitive to ultraviolet (uv) light, the preliminary tests were performed using the third harmonic of a Ti:Sapphire laser.[13] The 265 nm light was generated by focusing an 800 nm, 26 fs, 3 mJ laser pulse in air with an f-30 lens. The uv beam was collimated using a second lens, and separated from the infrared light by a pair of prisms. Finally, the uv light was focused onto the photocathode of the streak camera. They demonstrate a time resolution of 800 fs at this wavelength. Two uv pulses were used for calibration purposes, which were obtained by inserting a known thickness glass plate into the beam before focusing the uv onto the photocathode. The theoretical time resolution of the camera at this wavelength is not clear, since the photoelectron energy distribution of the photocathode at this wavelength is not available. From our uv tests, we found that the dynamic spatial resolution in the scanning direction deteriorates with increasing sweep speed. However, this could be corrected by readjusting the focusing current. We also found that the sweep speed of the camera could not be increased beyond a certain point, because the electron path was then obstructed by the plates. This occurred because the speed of the electron bunch through the deflection region does not perfectly match the speed of the voltage pulse in the deflection plates in the propagation direction. After this test, we redesigned the deflection plates, with which we obtained 0.54 ps resolution, as shown in Fig. 3.

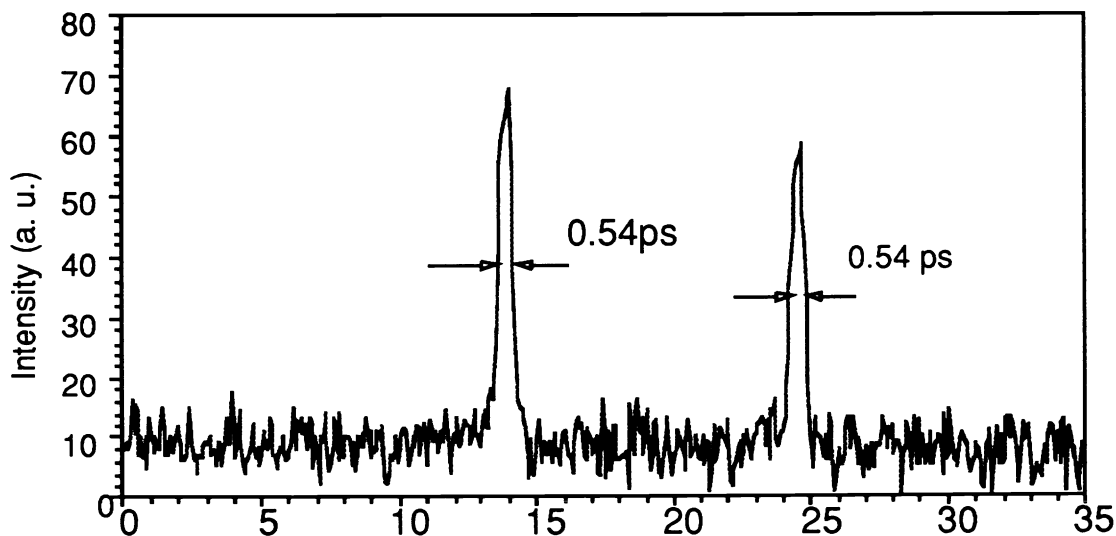


Figure 3: Streak camera time resolution measured using 15 fs uv pulses at 2650 Å.

To test the time resolution of the camera in the x-ray and xuv region, we used the fastest x-ray pulses available to date, which are high harmonics generated by a 25 fs Ti:sapphire laser.[4] A 2 - 20 mJ laser pulse was focused into a gas cell filled with Ar gas. The backing pressure for the gas cell was 8 Torr. The generated high harmonics were monochromatized using an x-ray spectrometer (HREF-SXR-1.75, Hettrick Scientific). We used a single high harmonic signal centered at $\approx 170 \text{ \AA}$ for the streak camera calibration. The pulse duration of the high harmonics is believed to be significantly shorter than the 26 fs laser pulse itself. However, dispersion introduced by the x-ray spectrometer broadens the x-ray pulse to 300 fs. Using these high harmonics, we obtained a time resolution of 880 fs in the x-ray region for our streak camera, as shown in Fig 4. This is, to our knowledge, the first demonstration of a sub-ps response x-ray streak camera. Our results are somewhat longer than the expected 0.6 ps response calculated from a convolution of the dispersed x-ray pulse duration ($\approx 0.3 \text{ ps}$) and estimated camera resolution ($\approx 0.5 \text{ ps}$). We believe that the difference is due to the decrease of spatial resolution in the dynamic or streaked mode. Further work is in progress to improve on these initial results, by designing better electrically matched streak plates, and by using low-jitter photoconductive switches to trigger the streak camera.[12]

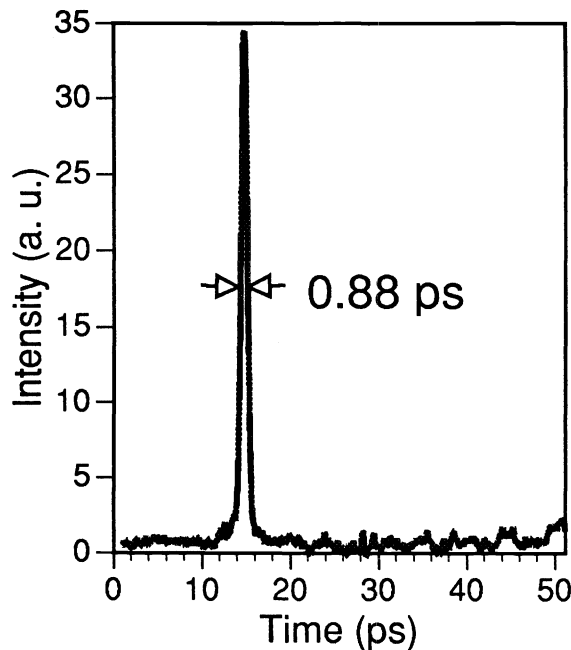


Fig. 4 Time resolution for 170A signal

In conclusion, we have demonstrated a novel design x-ray streak camera with sub-picosecond time resolution. Sub-20 fs high harmonics generated by a 25 fs laser were used to calibrate our streak camera. We believe that the time resolution our camera for X-ray can be improved further by using the redesigned tube. Our work demonstrates that sub-picosecond time resolution experiments can be performed in a straightforward manner using currently available synchrotron or laser-plasma sources.

4. Acknowledgments

This work was supported by the National Science Foundation, by the Air Force Office of Scientific Research, and by the Chinese Science and Technology Committee. The authors gratefully acknowledge the assistance of Hou Xun. Zenghu Chang acknowledges fellowship support from the Chinese Academy of Sciences. Henry Kapteyn acknowledges support from a Sloan Foundation Fellowship. Z. Chang is on leave from Xi'an Institute of Optics and Precision Mechanics, P. R. China

5. References

1. M. M. Murnane, H. C. Kapteyn, M. D. Rosen, R. W. Falcone, *Science* **251**, 531 (1991).
2. A. L'Huillier, P. Balcou, *Phys. Rev. Lett.* **70**, 774 (1993).
3. J. J. Macklin, J.D. Kmetec, C.L. Gordon III, *Phys. Rev. Lett.* **70**, 766, (1993)
4. J. Zhou, J. Peatross, M. M. Murnane, H. C. Kapteyn, I. P. Christov, *Phys. Rev. Lett.* **76**, 752 (1996).
5. M. M. Murnane, H. C. Kapteyn, R. W. Falcone, *Appl. Phys. Lett.* **56**, 1948 (1990).
6. R. Shepherd, R. Booth, D. Price, M. Bowers, D. Swan, J. Bonlie, B. Young, J. Dunn, B. White, R. Stewart, *Rev. Sci. Instrum* **66**, 719 (1995).
7. J. M. Schins, P. Breger, P. Agostini, R. C. Constantinescu, H. G. Muller, G. Grillon, A. Antonetti, A. Mysyrowicz, *Phys. Rev. Lett.* **73**, 2180 (1994).
8. J. P. Zhou, C. P. Huang, M. M. Murnane, H. C. Kapteyn, *Opt. Lett.* **20**, 64 (1995).
9. G. L. Stradling, J. K. Stuebaker, C. Cavailler, J. Launspach, J. Planes, *SPIE*, (Bellingham, WA, 1986).
10. D. J. Bradley, A. G. Roddie, W. Sibbett, M. H. Key, M. J. Lamb, C. L. S. Lewis, P. Sachsenmaier, *Opt. Comm.* **15**, 231 (1975).
11. B. L. Henke, J. Liesegang, S. D. Smith, *Phys. Rev. B* **19**, 3004 (1979).
12. G. A. Mourou, W. Knox, *Appl. Phys. Lett.* **36**, 623 (1982).
13. S. Backus, J. Peatross, M. Murnane, H. Kapteyn, *Opt. Lett.* **21**, 665 (1996).